# Application of CFD in the Design of Flow Control Concepts for a Ducted-Fan Configuration

W. Kelly Londenberg
Sr. Aircraft Design Analyst
AVID LLC
Yorktown, VA
kelly.londenberg@avidaerospace.com

O. John Ohanian, III
Aircraft Design Engineer
AVID LLC
Blacksburg, VA
john.ohanian@avidaerospace.com

## ABSTRACT

Leading and trailing edge flow control concepts were investigated for control of small ducted-fan unmanned aerospace vehicles. These concepts have the potential to augment vehicle controllability while decreasing dependence on conventional control surfaces. Steady state and unsteady CFD analyses were utilized in the design and analysis of Synthetic Jet Actuators, narrowing the concepts that were built and wind tunnel tested. Steady state analyses of leading-edge blowing concepts oriented 45° against the local flow, 5° inside the duct lip created a 60% change in pitching moment. Unsteady analyses of trailing edge blowing concepts revealed that blowing can significantly affect the flow over the Coanda trailing-edge surface. When the vehicle is at an angle of attack, partial circumferential blowing resulted in nearly the same effects on pitching moment as full circumferential blowing, thereby reducing experimental fabrication costs. Both of these predicted effects were later verified in wind tunnel testing.

## INTRODUCTION

A ducted fan has more thrust than an isolated fan at the same diameter and power due to the high-speed flow over the duct lipand the elimination of tip loses. This high-speed induced flow creates a low-pressure region over the duct lip, resulting in a pure axial force in hover. In forward fight the duct lip contribution results inaxial and normal forces coupled with a pitching moment. By controlling the separation of the flow over the duct lip, control moments may be generated with sufficient strength to overcome moments due to wind gusts. Conversely, the capability to maintain attached flow in conditions susceptible to separation may lead to performance gains. Micro unmanned aerospace vehicles (UAVs) need to have controls that are cheaper and more reliable, and require less volume, weight and power as things get smaller. AVID LLC has been investigating alternative concepts for controlling the ducted fan.[1,2]

The compact nature of synthetic jet actuators provides a capability for small UAVs to manage the flow state via a zero-net-mass-flux jet. At the duct lip, the asymmetric utilization of the jets would result in a flow separation, decreasing the normal forces over the separated lip, with corresponding control moments created, Figure 1. Blowing over the duct trailing edge could also enhance vehicle controllability by maintaining attached flow over a Coanda trailing edge surface. Likewise, differential, or asymmetric blowing control would result in increased surface normal forces over the surface with attached flow, with an accompanying moment, Figure 2.

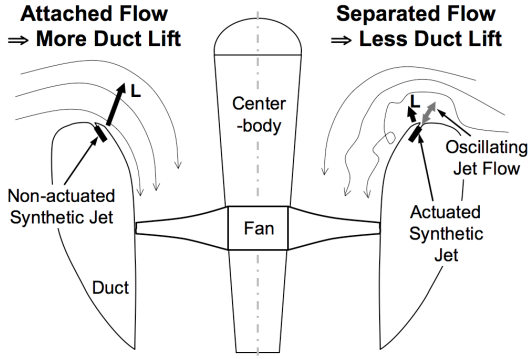


**Figure 1. Asymmetric blowing can result in control moment creation.**

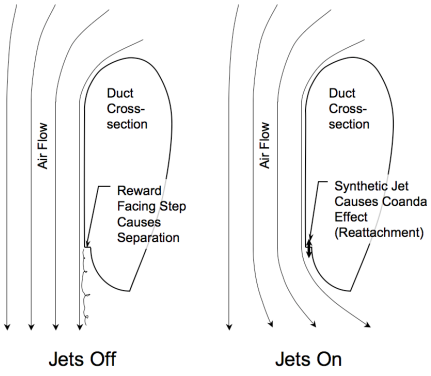


**Figure 2. Blowing over a Coanda trailing edge surface maintains attached flow.**

Presented at the International Powered Lift Conference, October 5-7, 2010, Philadelphia, PA. 

While the synthetic jet actuator (SJA) hardware can be designed and evaluated using empirical data, lower order methods, and bench testing, show that blowing has a non-linear effect on a the ducted fan aerodynamics. In addition, to fully model the effect of the SJAinduced flow, the periodic nature of the jet should be modeled. This paper describes the use of unsteady CFD for the analysis and optimization of SJA for circulation control on a small, ducted fan vehicle.

## METHODOLOGY

The FUN3D[3] unstructured-grid flow solver was used as the analysis tool in this study. This code solves the incompressible, Euler, or Reynolds-averaged Navier-Stokes equations using a node-centered, up-wind, finite volume scheme. The Spalart and Allamaras[4] (SA) one-equation turbulence model as well as several two-equation k-omega and k-epsilon models and a hybrid large eddy simulation model are available for computation of turbulence quantities. The SA model may be either tightly or loosely coupled with the flow equations. In this study, the FUN3D code is run incompressible, using the loosely coupled SA turbulence model.

Effects of a rotor are incorporated into the flow solver via source terms.[6] The source terms result from an actuator disk model that uses the computed velocities as inflow. Several blade-loading models are available, with the blade-element-loading model used in the current work.

Unstructured tetrahedral meshes were constructed using GridTool[7] and Vgrid.[8] The meshes generated are full tetrahedral with the boundary layer portions of the grid constructed using an advancing layer technique and advancing front method used outside of the boundary layer.

## GRID GENERATION

An unstructured mesh was constructed about a ducted fan configuration as shown in Figure 3. The outer boundaries are set 20 duct diameters away. Since the ducted fan is primarily a hovering vehicle, fan exit velocity dominates the flowfield and was used as the velocity scale in computing y+. Using this velocity as the reference velocity, surface spacing was targeted to yield y+ ≈ 1 at the first points off the surface inside the duct.

The FUN3D rotor model solves for the fan blade loading on an arbitrary Cartesian mesh, and then interpolates the rotor influence into the computational grid.[5] To minimize interpolation errors, the cell sizes of the Cartesian mesh and the computational mesh should be similar. In practice, it has been found that a 100 radial x 720 normal Cartesian mesh is sufficient for the actuator disk computations.

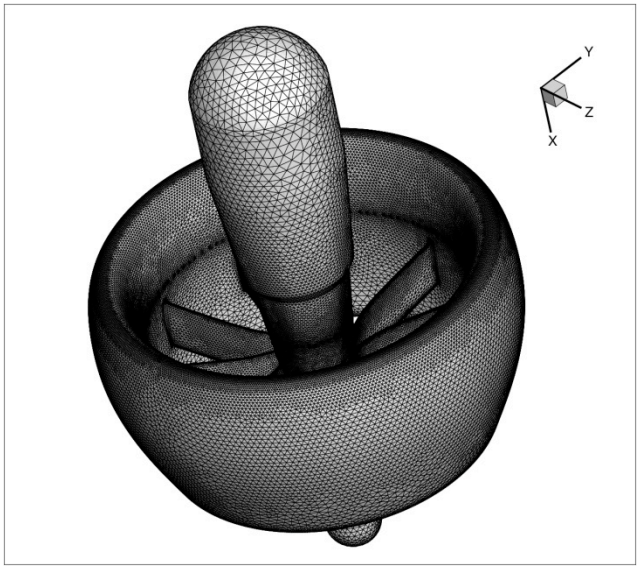


**Figure 3. Surface mesh about a ducted-fan vehicle.**

## CIRCULATION CONTROL ANALYSES

*BASELINE ANALYSIS*

Incompressible solutions were obtained for the ducted fan configuration at 15-knots and 14.33° tilt from vertical (-14.33° angle of attack) at 2,200 feet altitude, Figure 4. The fan was simulated as an actuator disk, using the rotor method integrated with the FUN3D solver. Using blade geometry and airfoil aerodynamics, this actuator disk method iterates the swirl and pressure increase due to the fan with the computed inflow, resulting in a good simulation of first order fan effects.

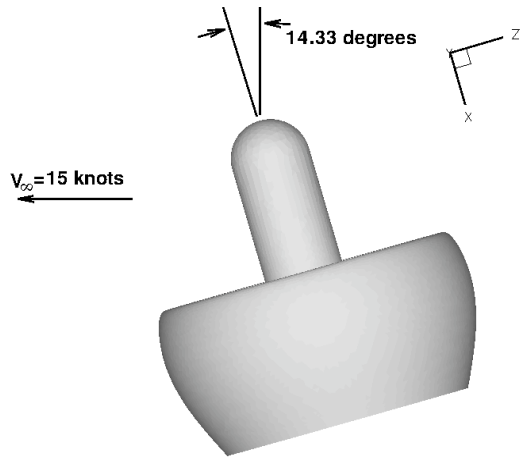


**Figure 4. Circulation control analyses and design conducted for ducted fan at 2,220 ft and 15-kts forward flight.**

Pressure and velocity contours resulting for the solution of the baseline duct configuration, Figure 5 through Figure 8, show attached flow over the windward and leeward sections. At the 15-knot cruise condition, there is a significant acceleration of the flow over the windward lip, resulting in large suction pressures creating a lift force and pitching moment. The acceleration is not as significant, nor the suction pressures as high over the lip at the leeward section, Figure 7 and Figure 8.

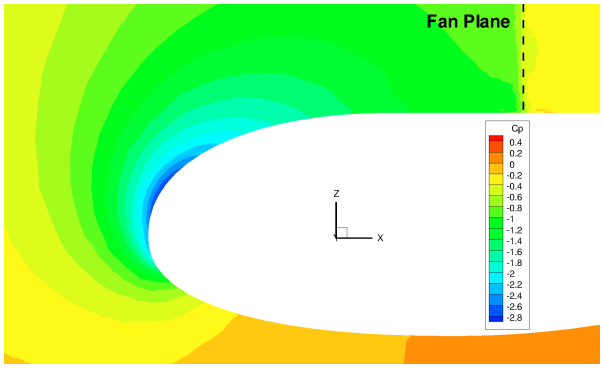


**Figure 5. Lower surface pressures are predicted over the windward duct lip at the 15-kt cruise condition.**

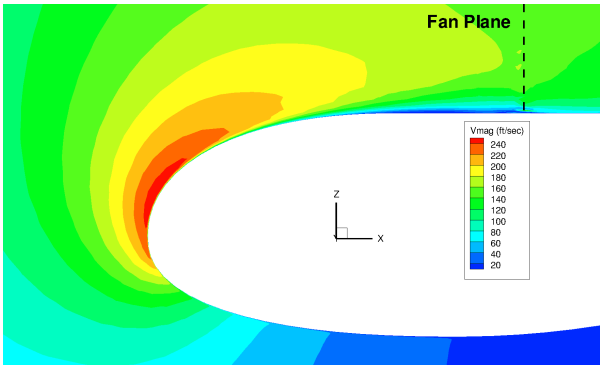


**Figure 6. Accelerated flow is predicted over windward lip at the 15-kt cruise condition.**

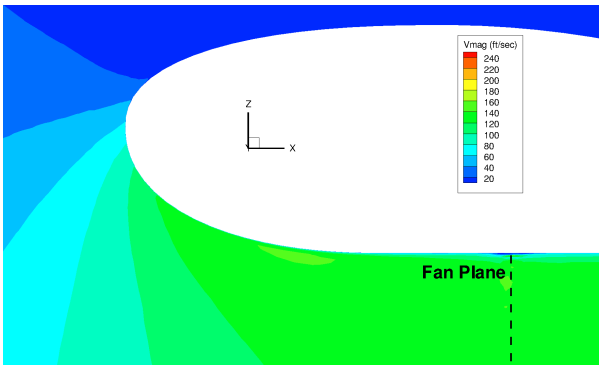


**Figure 7. Flow over the leeward duct lip is dominated by fan-induced flow at the 15-kt cruise condition.**

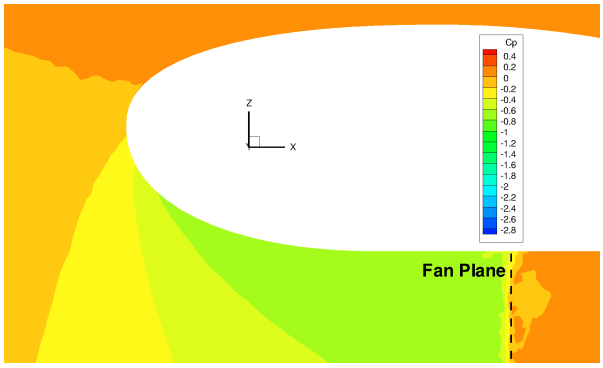


**Figure 8. Leeward duct lip surface pressures show little effect of fan-induced flow at 15-kt cruise**

*LEADING-EDGE BLOWING ANALYSIS*

Initially, leading-edge blowing was evaluated for a jet blowing from a 0.04" step, directed5 deg into the duct, the "40-5" configuration (see Figure 11, duct windward side, and Figure 13, duct leeward side).Three blowing conditions were analyzed: no blowing, steady 150 ft/sec slot normal velocity for the bottom half of the duct (windward), and steady 150 ft/sec step normal velocity along the upper half (leeward) of the duct. The addition of the 40-5 step significantly reduces the lip suction over the bottom windward section, Figure 9, but has very little effect on the upper leeward section, Figure 10. However, the 150-ft/sec blowing out of the step cannot return the performance to that of the baseline duct, as seen in Figure 9. Examination of the velocity and pressure contours, Figures 11 and 12, further shows that the blowing for the 40-5 configuration produces only a localized effect.

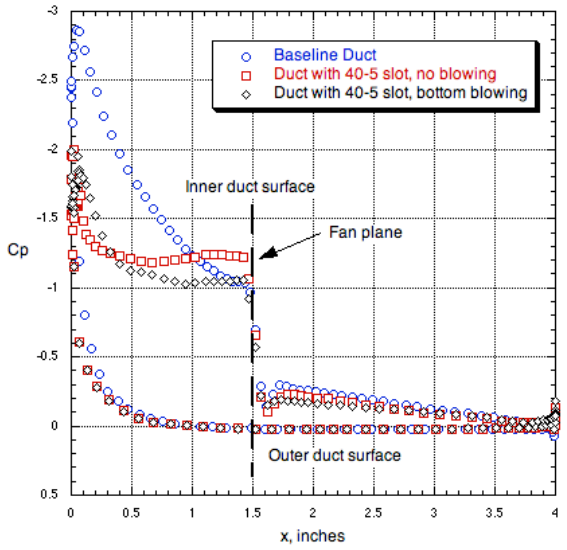


**Figure 9. Steady 150 ft/sec blowing has little effect on windward lip surface pressures at the 15-kt cruise condition.**

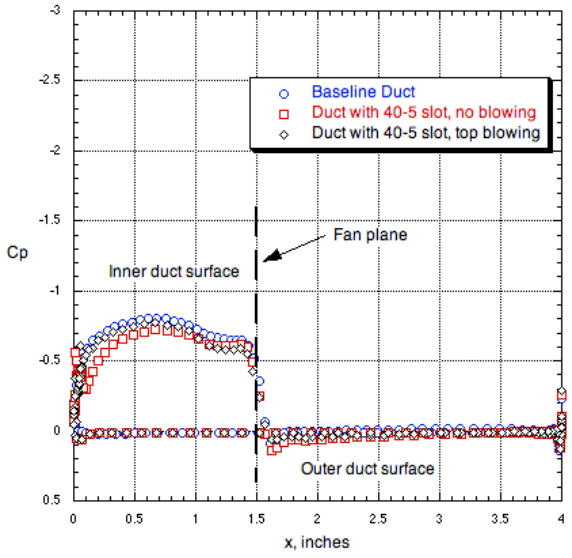


**Figure 10. The presence of the step with and without blowing has little effect of leeward duct lip surface pressures.**

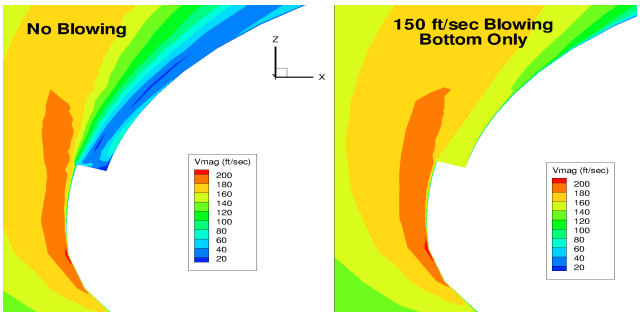


**Figure 11. Leading-edge blowing has only localized effect on windward duct lip at 15-kt cruise condition.**

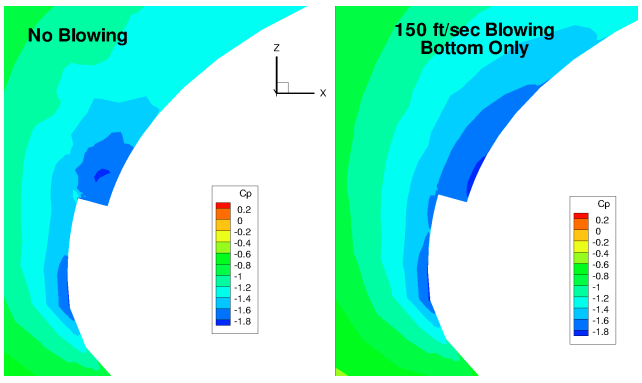


**Figure 12. Windward duct lip blowing has only localized effect on surface pressures at 15-kt cruise conditions.**

Examination of the pressures resulting from blowing along only the upper half of the duct, Figure 10, reveals that blowing along the leeward side of the duct has almost no effect on the computed pressures. This is also evident in the computed pressure coefficient contours, Figure 13, and in the computed velocity contours, Figure 14. This region of the duct lip does not contribute much to the lift and pitch moment of the vehicle in forward flight.The trends observed in the pressure comparisons are also seen in comparisons of the predicted forces and pitching moment on the ducted fan, Table 1. The pitching moment is referenced to a point along the centerline, one inch aft of the duct lip (the quarter chord of the duct). The step geometry significantly reduces the pitching moment by nearly 40% when compared to the baseline duct lip without step geometry. With 150-ft/sec blowing velocity along the bottom half of the duct, 9.8% of the difference between baseline and non-blowing pitching moment is recovered. Referencing to the non-blowing step as the baseline, blowing along the bottom, windward, half of the duct, in cruise flight, results in an additional 6% nose-up pitching moment. Blowing out the top, leeward, half of the step only produced an additional 1.5% nose-up pitching moment.

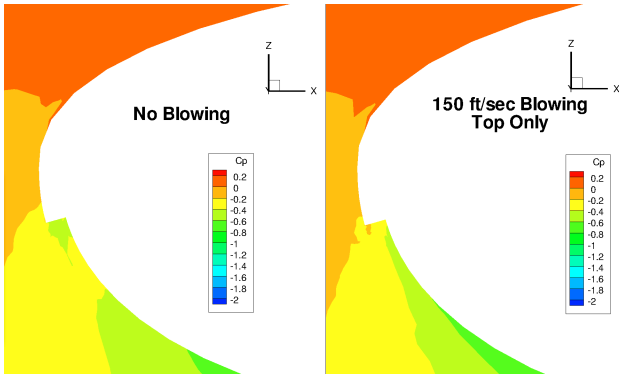


**Figure 13. Steady blowing over leeward duct lip had only minimal effect of predicted surface pressures at 15-kt cruise condition.**

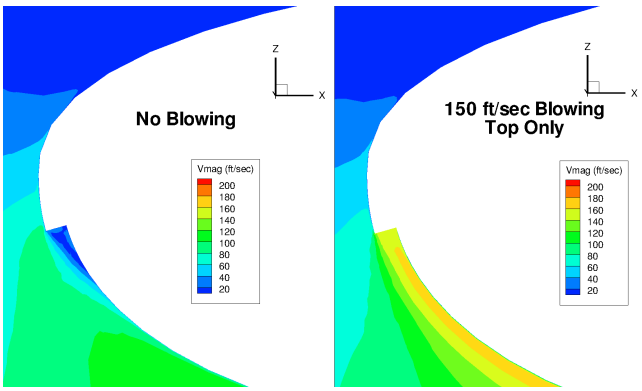


**Figure 14. Steady blowing over leeward duct lip decreased the effect of the step.**

| | Lift (lbs) | Drag (lbs) | Pitching Moment (ft-lbs) | Duct Thrust (lbs) | Fan Thrust (lbs) | Total Thrust (lbs) |
|---|---|---|---|---|---|---|
| **Baseline** | 3.71 | -0.42 | 0.2923 | 3.49 | 3.40 | 6.89 |
| **No Blowing** | 2.70 | -0.32 | 0.1807 | 2.54 | 3.85 | 6.39 |
| **Windward Blowing** | 2.72 | -0.26 | 0.1916 | 2.56 | 3.91 | 6.47 |
| **Leeward Blowing** | 2.78 | -0.21 | 0.1835 | 2.64 | 3.80 | 6.44 |

**Table 1: Predicted Force and Moments**

For insight into what is occurring, we refer back to the velocity contours over the windward lip of the baseline vehicle (Figure 11). In the region where the step was introduced, the velocities over the baseline lip were in the realm of 240 ft/sec. This high-speed flow, and consequently high dynamic pressure, reduces the static pressure on the duct lip, causing lift and pitching moment. A jet velocity of 150 ft/sec simply cannot impart the needed velocity to achieve these static pressure levels. While peak synthetic jet velocities have been reported in the realm of 420 ft/sec, the mean jet velocity is usually much lower (by a factor of two to four). Using synthetic jets in a lower speed region of the duct lip is anticipated to be more effective.

Another possible explanation for the lack of effectiveness of blowing in the current case is that the blowing was primarily inside the duct lip. The flow over the lip is dominated by the induced fan flow. The velocity contours shown in Figures 11 and 14 reveal that there are similar velocity levels over the duct lip with and without blowing, for both the top and bottom of the duct. The only effect of blowing is to re-energize the flow as it separates over the slot step. Blowing outside of the duct may be more effective in that it could be used to accelerate the flow over the lip.

Based upon these analyses, a new duct design was developed that would allow blowing over the outside duct surface, aligned against the local flow direction, Figure 15, with the idea that the blowing velocity would separate the flow over the lip. Multiple orientations were analyzed as presented in Table 2. The configuration oriented 45° against the local flow direction (*beta=45°, or b45)*, 5° inside the lip, (*alpha=5°, or a5)* resulted in the greatest effectiveness. For this configuration, *a5b45*, three blowing velocities were analyzed: 50-ft/sec, 100-ft/sec, and 200-ft/sec. Comparing the 100-ft/sec and 200-ft/sec blowing with the no blowing case, Figure 16, shows that leading-edge blowing is separating the flow over the lip as intended. As blowing velocity is increased, the core of the separated region is lifted farther off the surface. Similar effect of blowing is seen in wind tunnel flow visualization, Figure 17. Also, as blowing velocity is increased, the effect on the vehicle pitching moment is increased. The 50-ft/sec blowing velocity reduced the pitching moment by more than a third compared to the no blowing configuration, 100-ft/sec blowing reducing it by half, and 200-ft/sec blowing by two thirds, Table 3. An interesting observation is that the difference in pitching moment between full (360°) blowing and windward blowing (front 180°) was minimal, implying that the majority of the effect on the flow is happening at the windward lip. Blowing over the leeward half alone produced little effect.

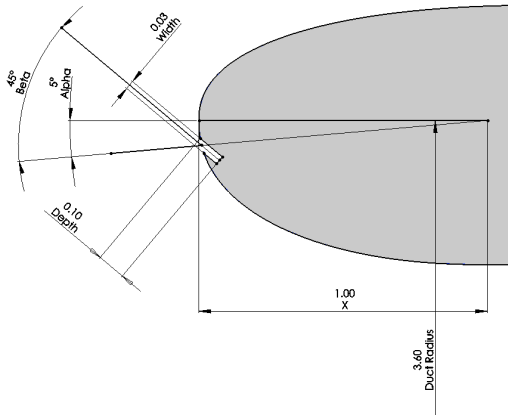


**Figure 15. The alpha and beta parameters define the location and orientation, respectively, of the lip duct, shown for the leeward side.**

| | Jet Blowing Velocity (fps) | Lift (lbs) | Thrust (lbs) | Pitching Moment (ft-lbs) | Pitching Moment Delta (%) |
|---|---|---|---|---|---|
| **baseline** | N/A | 3.71 | 6.89 | 0.2923 | 0.00 |
| **a-10b80** | 0 | 3.28 | 6.02 | 0.2840 | -2.84 |
| **a-10b80** | 50 | 3.21 | 5.98 | 0.2784 | -4.75 |
| **a-10b80** | 75 | 3.17 | 5.96 | 0.2752 | -5.85 |
| **a-10b80** | 100 | 3.10 | 5.93 | 0.2693 | -7.87 |
| **a-20b-20** | 50 | 4.04 | 7.52 | 0.3184 | +8.93 |
| **a5b45** | 0 | 2.89 | 5.51 | 0.2575 | -11.91 |
| **a5b45** | 50 | 2.27 | 5.07 | 0.1595 | -44.43 |
| **a5b45** | 100 | 2.04 | 4.90 | 0.1193 | -59.19 |

**Table 2: The s5b45 slot geometry had the largest effect on vehicle pitching moment.**

Since the a5b45 leading-edge slot geometry exhibits at least a 50% reduction in pitching moment for even for moderate steady state blowing, this geometry was identified for further evaluation with wind tunnel testing.

| Blowing Type | Jet blowing velocity (fps) | Lift (lbs) | Pitching Moment (ft-lbs) | Pitching Moment Delta (%) |
|---|---|---|---|---|
| **None** | 0 | 2.89 | 0.2575 | N/A |
| **Full** | 50 | 2.27 | 0.1595 | -38.06 |
| **Windward** | 50 | 2.27 | 0.1620 | -37.09 |
| **Leeward** | 50 | 2.89 | 0.2511 | -2.49 |
| **Full** | 100 | 2.04 | 0.1193 | -53.67 |
| **Windward** | 100 | 2.05 | 0.1267 | -50.80 |
| **Leeward** | 100 | 2.89 | 0.2522 | -2.06 |
| **Full** | 200 | 2.07 | 0.0875 | -66.02 |
| **Windward** | 200 | 2.02 | 0.1139 | -55.77 |
| **Leeward** | 200 | 2.97 | 0.2383 | -7.46 |

**Table 3: Full blowing resulted in little additional pitching moment over windward half blowing.**

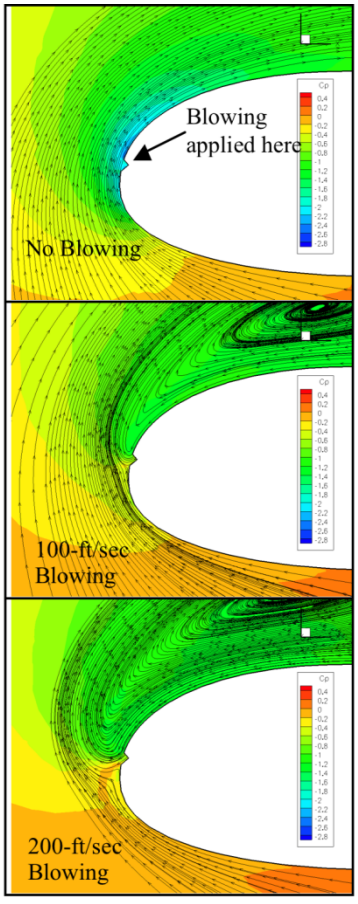


**Figure 16. The a4b45 leading-edge flowing geometry results in separated flow over the lip.**

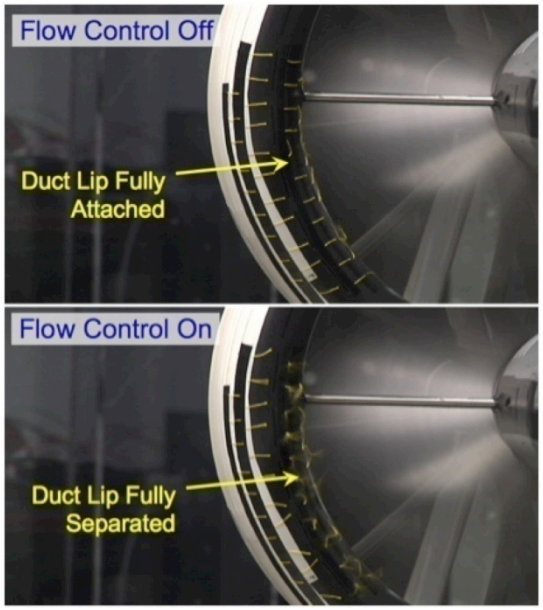


**Figure 17. Experiment shows similar effects of leading edge blowing: (top) no blowing, (bottom) steady blowing at highest rate.**

*COANDA TRAILING EDGE SURFACE ANALYSIS*

A trailing edge geometry was developed for a 0.06-inch step height and trailing edge radius of curvature of 1.0-inch, Figure 18. In initial steady-state analyses, the jet velocity was imposed at the slot exit plane, i.e., the internal slot geometry was not modeled. Steady-state analyses of the full-scale vehicle revealed that the combination of reducing the step height and increasing the trailing edge radius of curvature resulted inconditions that allow the flow to remain attached over the complete trailing edge for a 200-ft/sec blowing velocity over the windward half of the duct, Figure 19. Also evident in Figure 19 is the expansion of the streamtube aft of the duct, biasing it toward the windward side. The effect of the attached flow over the windward trailing edge is evident in the forces and moments,Table 4. Blowing over the windward trailing edge at 200 ft/sec decreased the pitching moment by a third. Although the expansion of the streamtube resulted in an expected loss of thrust, power required decreased faster, resulting in an increase in duct figure-of-merit as compared to the case with no blowing. This represents an improvement in propulsive efficiency. Blowing over the leeward side alone resulted in an almost 40% increase in pitching moment, and a decrease in duct figure-of-merit.

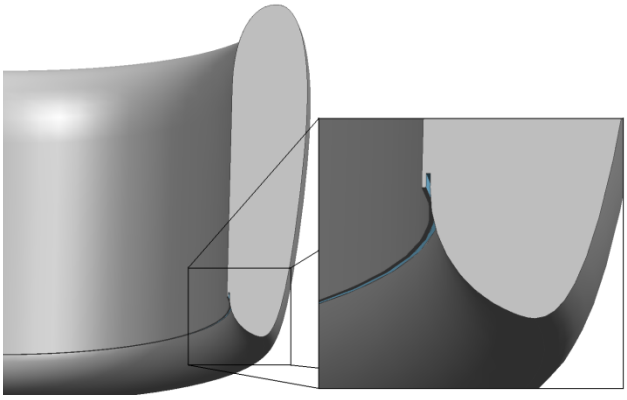

**Figure 18.Coanda trailing edge geometry with 0.06-in step and 1.0-in radius of curvature.**

| Blowing | Jet Blowing Velocity (fps) | Thrust (lbs) | Power Required (HP | FOM | Pitching Moment Delta (%) |
|---|---|---|---|---|---|
| None | 0 | 5.46 | 0.76 | 0.74 | N/A |
| Full | 200 | 5.00 | 0.63 | 0.78 | 1.95 |
| Windward | 200 | 5.12 | 0.66 | 0.75 | -34.71 |
| Leeward | 200 | 5.12 | 0.72 | 0.70 | 39.92 |

**Table 4: 200 ft/sec Coanda blowing reduces pitching moment by a third.**

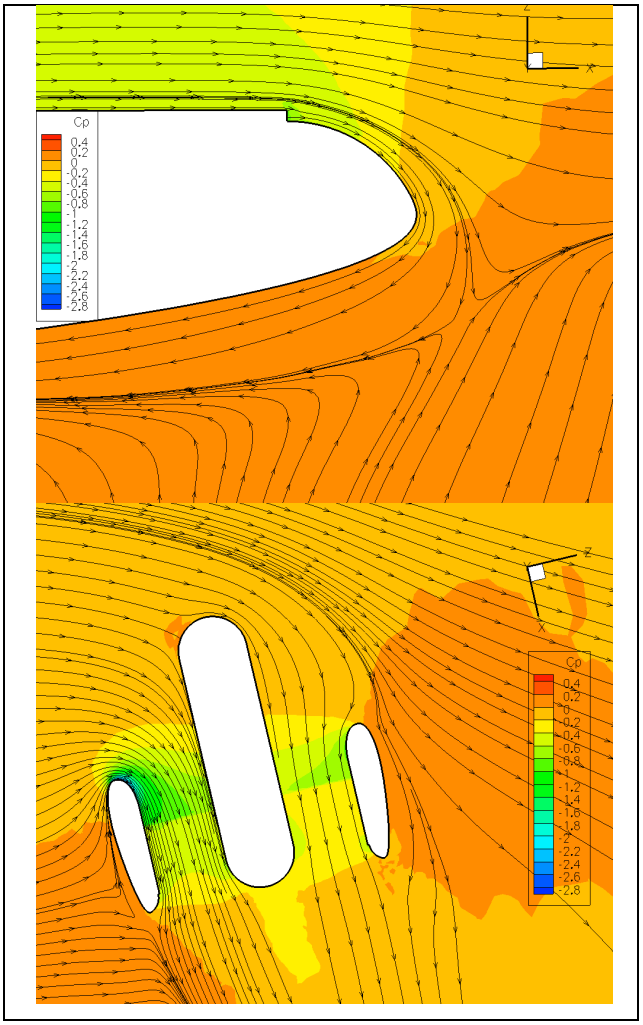


**Figure 19. The flow remains attached over 0.5-in radius Coanda surface with 0.04-in step and 200 ft/sec blowing velocity**

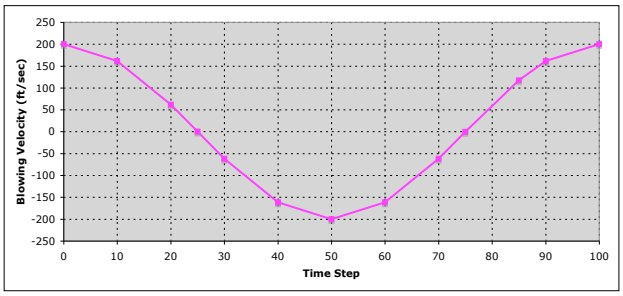


**Figure 20.Jet blowing is modeled as a cosine function over 100 time steps**

*UNSTEADY COANDA TRAILING EDGE SURFACE BLOWING ANALYSIS*

To better understand the effects of a synthetic jet on the forces and moments ona ducted fan vehicle, higher-order modeling of the jet in the computational analysis was initiated. To begin, the geometry was improved to include the jet slot depth, modeling the jet plenum to the synthetic jet orifice. In addition, the jet velocity imposed as a boundary condition at the synthetic jet orifice plane was modeled as a time varying sinusoidal function. The 2400-Hz, ±200-ft/sec normal velocity boundary condition (values taken from bench test performance) was modeled over 100 computational time steps, as shown in Figure 20, plotted using twelve of the 100 time steps.

After seven blowing cycles, a time history of one cycle is presented in Figure 21 showing plots of pitching moment and thrust. Here, pitching moment and thrust are plotted against jet velocity for one blowing cycle over the time steps depicted inFigure 20. The data points for 200-ft/sec, or the

first and one-hundredth time step in the cycle, lying on top of each other is an indication of solution convergence. The average of the forces and moments over this last cycle, compared with the baseline case and steady-state blowing case (all at wind tunnel model scale), reveal that the effectiveness of the jet on pitching moment is decreased by time varying blowing, Table 5. Analysis of snap-shots of the flow field near the duct windward side trailing edge during the blowing cycle, Figure 22, provides insight into what is causing the decrease in pitching moment effectiveness.

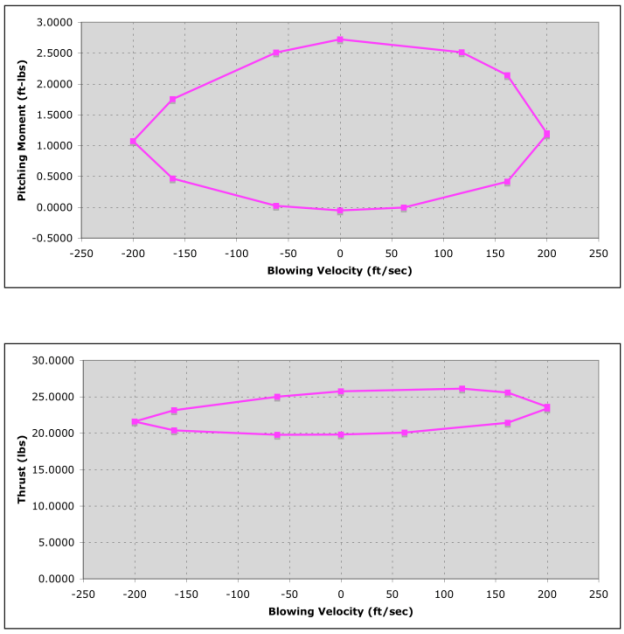


**Figure 21. Time history plot indicates that the unsteady solution is converged.**

| Configuration | Pitching Moment (ft-lbs) | Thrust (lbs) |
|---|---|---|
| **Baseline** | 1.55 | 23.52 |
| **Steady Blowing** | 1.03 | 22.34 |
| **Unsteady Blowing** | 1.23 | 22.74 |

**Table 5: Time varying blowing results compared to baseline and steady blowing at wind tunnel scale.**

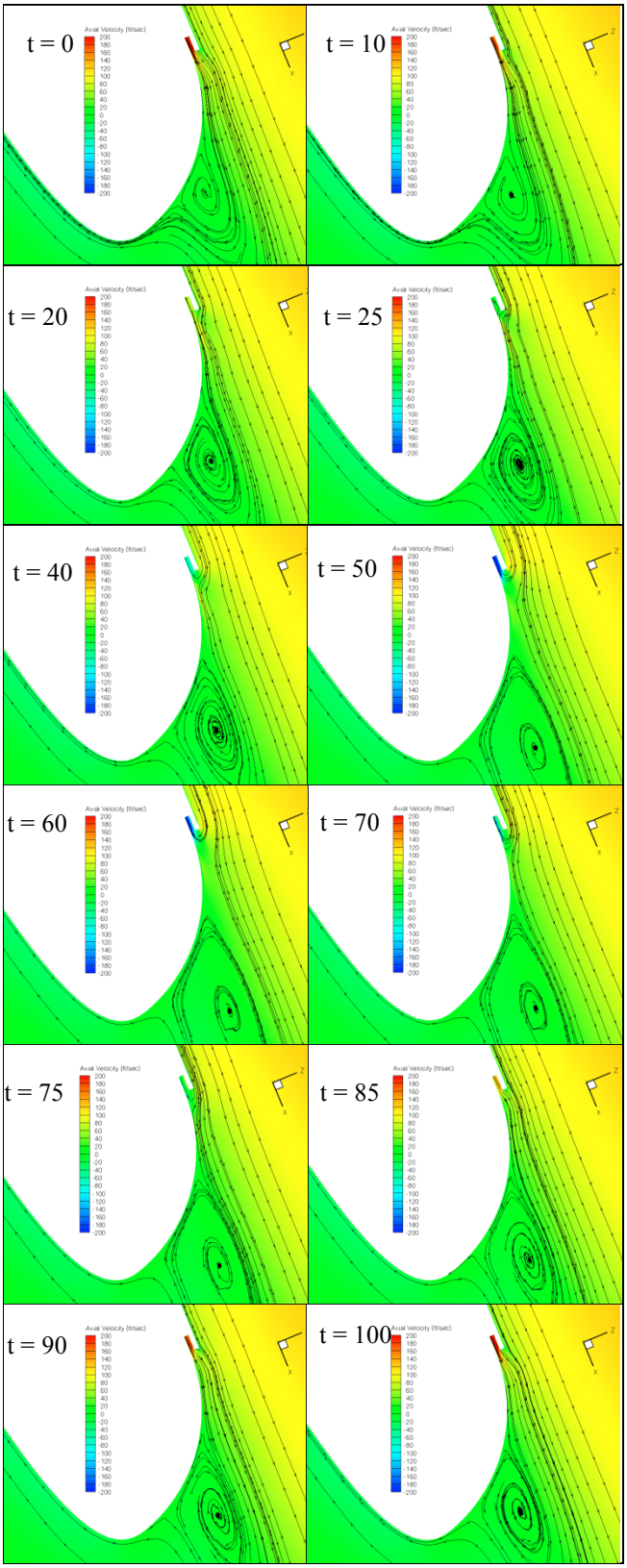


**Figure 22. The flow is detaching and reattaching to the Coanda surface with time varying blowing, 200 ft/sec amplitude. One period is displayed for windward side.**

In Figure 22, the velocity streamlines, which are superimposed on axial velocity contours, show the flow rolling up aft of the duct windward side trailing edge. Note, that at the maximum actuator in-stroke, t=50, the flow over top of the slot is lifting off of the surface and is detaching from the Coanda trailing edge surface earlier. Even though the mean flow is attached, examination of the steady-state blowing solution, Figure 23, reveals an unstable region aft of the duct trailing edge, indicated by the saddle-point in the streamlines. This separation in the unsteady blowing may be a result of the sharp edges of the slot, sensitivity to jet velocity, or both. Based upon these findings for the forward flight case, geometry was developed with a filleted corner outside the slot exit where the duct flow and jet flow would meet. An analysis of the hover condition does show that flow stays attached to the Coanda trailing-edge surface with this improved geometry, Figure 24. This behavior can be qualitatively compared with the wind tunnel flow visualization, Figure 25. Based upon these analyses the filleted slot geometry was selected for the wind tunnel model geometry.

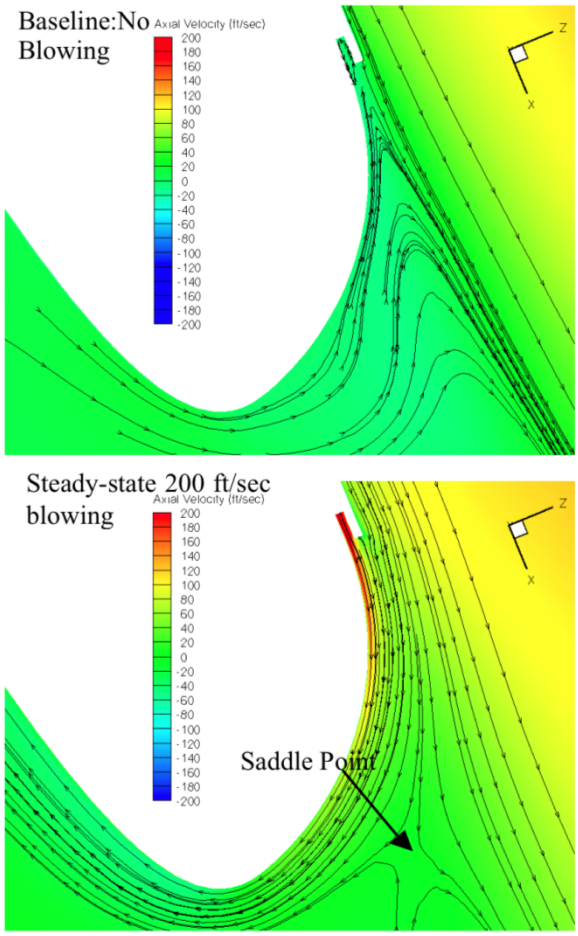


**Figure 23. Steady-state blowing exhibits saddle point in flow for 200 ft/sec jet normal velocity, windward side.**

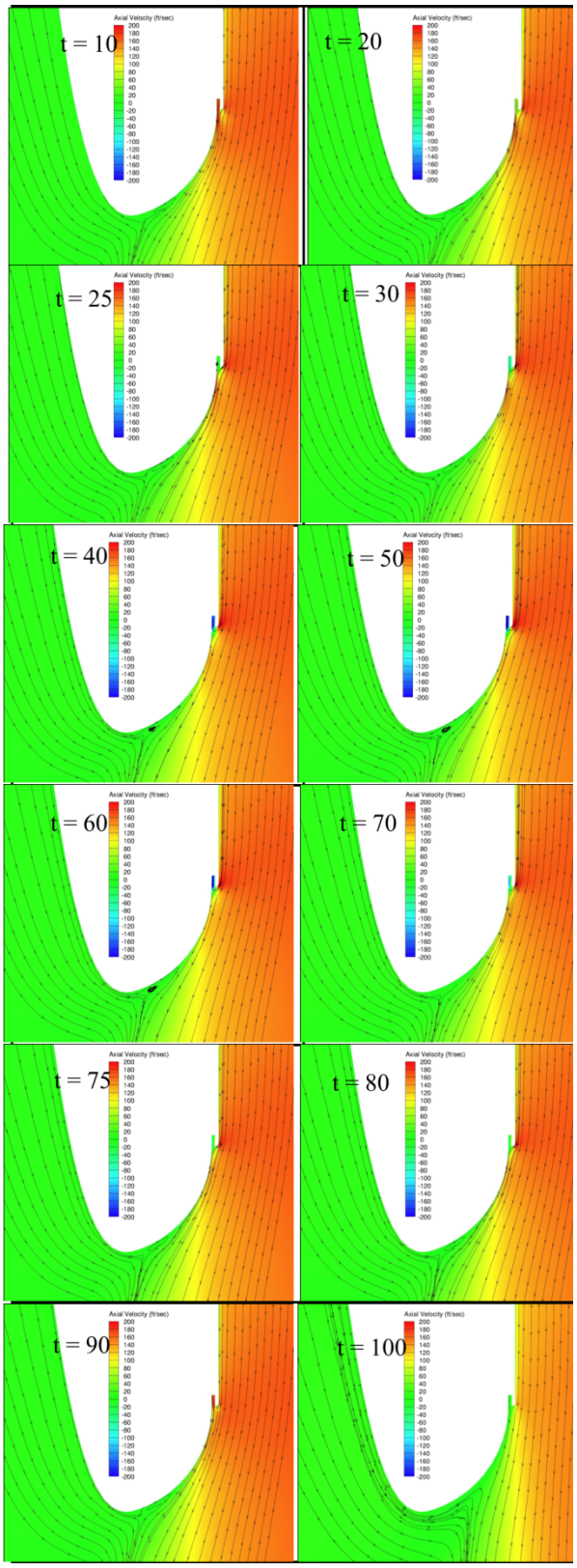


**Figure 24. Filleting the corner outside the windward slot exit stabilizes the flow over the Coanda trailing at hover conditions as seen in steam lines plotted over axial velocity contours. One period is displayed.**

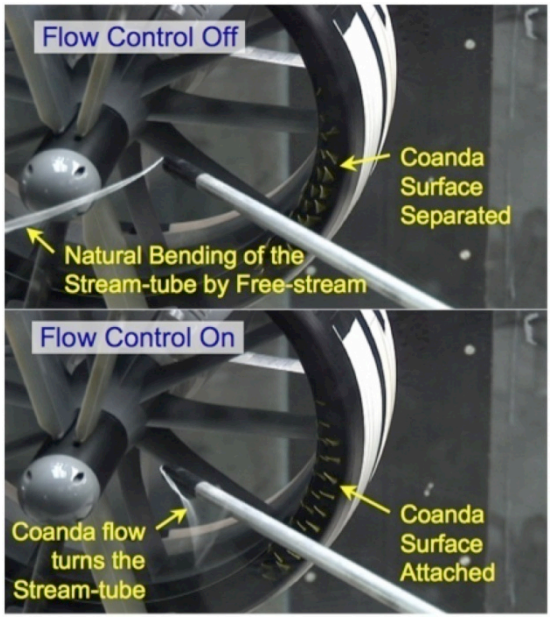


**Figure 25. Experiment shows similar effects of trailing edge blowing: (top) no blowing, (bottom) steady blowing at highest rate.**

## WIND TUNNEL MODEL DEVELOPMENT ANALYSES

During the development of wind tunnel hardware, several configuration design elements are required to be tested at reduced order. The selected leading-edge blowing geometry, a5b45, did not provide the required wall thickness for manufacturing of the wind tunnel model. The leading-edge shape was reduced to a5b35, a reduction from a 45° angle with the horizontal to a 35° angle to provide more wall thickness between the slot and the inner duct. The a5b35 geometry was analyzed computationally and found to result in 8% reduction in pitching moment effectiveness, compared with the no-blowing baseline case. The original geometry reduced pitching moment 57% while the new reduced pitching moment 49%.

To reduce model fabrication and instrumentation costs, synthetic jet actuators wereonly installed in a quarterof the trailing-edge circumference, centered about the windward side, Figure 26. Here, the view is looking upstream, through the duct, with the windward edge being the bottom of the duct. Computational analyses of the baseline, or no blowing condition, half circumferential blowing, and quarter circumferential blowing shows little difference in predicted wind-tunnel scale pitching moment and thrust between the quarter blown duct and half blown duct, Table 6. Both cases decrease pitching moment by a third. The half blown duct results in an additional half pound of thrust loss, due to the additional expansion of the streamtube aft of the duct; therefore only blowing a quarter may be beneficial. These analyses indicate that equipping only a quarter of the duct will not reduce the accuracy of the wind tunnel test.

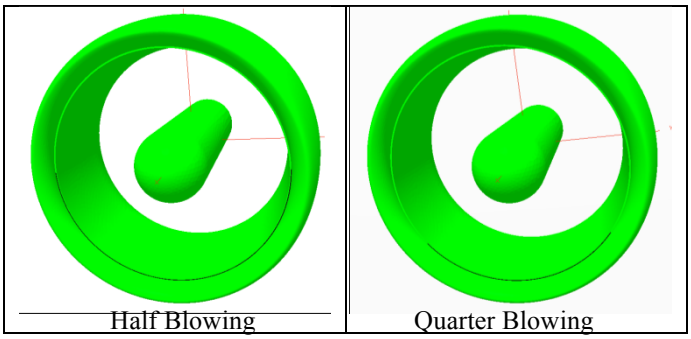


**Figure 26.Coanda blowing slot is centered about the windward edge.**

| Configuration | Pitching Moment (ft-lbs) | Thrust (lbs) |
|---|---|---|
| **Baseline** | 1.5323 | 23.5209 |
| **Quarter Blowing** | 1.0513 | 22.9167 |
| **Half Blowing** | 1.0340 | 22.3396 |

**Table 6: Blowing over a quarter of the Coanda trailing-edge had minimal affect on computed wind-tunnel scale pitching moment.**

## COMPARISON WITH EXPERIMENT

Experimental data showed that lower steady-state blowing velocities were more effective than a synthetic jet blowing velocity of the same average blowing velocity, Figure 27. To eliminate the velocity effects, pitching moment and figure-of-merit predictions for a series of steady-state blowing analyses in the hover condition are compared with an unsteady, 200 ft/sec blowing solution in Figure 28 and Figure 29, below. From these analyses it can be seen that the effect of the synthetic jet modeled as a time varying sinusoidal function with amplitude of 200 ft/sec is predicted as roughly equivalent to a steady-state blowing between 140 ft/sec and 150 ft/sec.

Analyses of higher blowing velocities has resulted in the predictions of non-physical flow fields, in particular, flow remaining attached completely around the circumference of the Coanda trailing-edge. Other researchers have seen similar results in the analysis of circulation control airfoil calculations [9,10]. These researchers noted non-physical jet wrap-around the Coanda trailing edge surface and attributed the feature to turbulence model, insufficient grid refinement, and / or the initial conditions used to start the unsteady solution. They suggested additional research in the numerics behind these solutions, research that is beyond the scope of the current project.

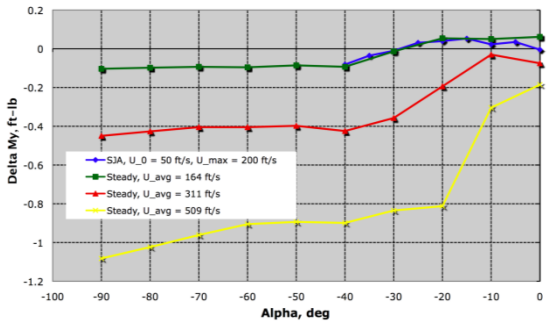


**Figure 27. Lower steady-state blowing velocities are more effective than comparable SJA average velocity.**

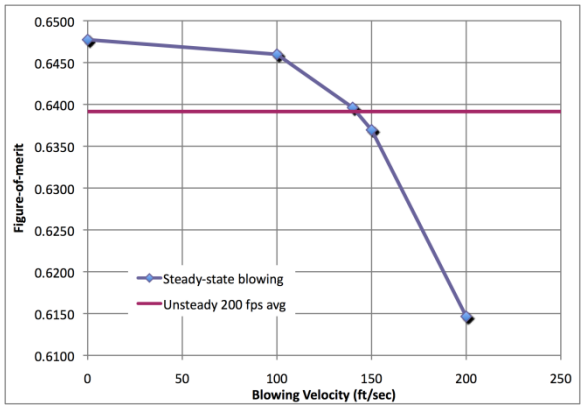


**Figure 28.Hover figure of merit resulting from 200 ft/sec unsteady SJA blowing is approximately equivalent to 150 ft/sec steady blowing level.**

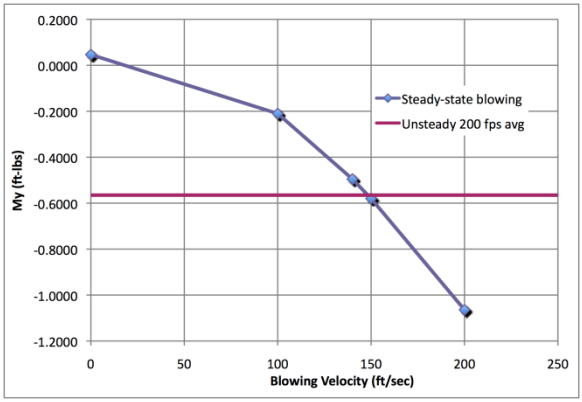


**Figure 29.Hover pitching moments created with 200 ft/sec unsteady SJA blowing are approximately equivalent to 150 ft/secsteady blowing.**

## CONCLUDING REMARKS

With the use of CFD early in the design of synthetic jet actuators, the effect of blowing concepts on the performance of a ducted fan vehicle was evaluated. Steady state analyses of numerous leading-edge concepts allowed for only the most promising concepts to be built and tested. Unsteady analyses of trailing-edge blowing over a Coanda surface resulted in refinement of the design, and indicated that blowing one quarter of the duct circumference yielded similar pitching moment control authority compared with halfcircumferential blowing. While the predicted leading-edge and trailing-edge effects of blowing are qualitatively similar to experimental flow visualization results, experimental blowing effectiveness was less than expected. Additional analysis indicated that higher peak velocities were required for the unsteady simulations to match the steady state blowing cases evaluated in the wind tunnel.

## ACKNOWLEDGMENTS

The authors thank the Air Force Research Laboratory (AFRL) for sponsorship of this research, specifically James D. Davis, the AFRL program manager of this Phase II SBIR contract. Also, thank you to colleagues at AVID LLC for theirtechnical support in conducting this research and in preparing this paper.The support and consultations provided by members of the Computational Aerosciences Branch at NASA Langley in applying FUN3D to this problem is gratefully appreciated.

## REFERENCES

[1] Ohanian, Osgar John, III, Karni, Etan D., Londenberg, W. Kelly, Gelhausen, Paul A., and Inman, Daniel J, "Ducted-fan Force and Moment Control via Steady and Synthetic Jets," AIAA Paper 2009-3622, 27th Applied Aerodynamics Conference, 22-25 June, 2009, San Antonio, TX.

[2] Bulgen, Onur, Kochersberger, Kevin B., Inman, Daniel J. and Ohanian, Osgar J., III, "Novel, Bi-Directional, Variable Camber Airfoil via Marco-Fiber Composite Actuators," AIAA 2009-2133, 50th AIAA/ASME/ASCE/AHS/ASC Structures, Structural Dynamics, and Materials Conference, 4-7 May 2009, Palm Springs, CA.

[3] Anderson, W. K., and Bonhaus, D.L., "An Implicit Upwind Algorithm for Computing Turbulent Flows on Unstructured Grids," *Computers and Fluids*, Vol. 23, No. 1, 1994, pp 1-22.

[4] Spalart, P.K. and Allmaras, S.R., "A One-Equation Turbulence model for Aerodynamic Flows," *La Recherche Aerospatiale,* No. 1., 1994, pp 5-21.

[6] O'Brien, D., *Analysis of Computational Modeling Techniques for Complete Rotorcraft Configurations,* Ph.D. thesis, Georgia Institute of Technology, 2006.

[7] Samareh, J. A.: "GridTool: A Surface Modeling and Grid Generation Tool", Proceedings of the Workshop on Surface Modeling, Grid Generation, and Related Issues in CFD Solutions, NASA Lewis Research Center, Cleveland, OH, NASA CP-3291, 1995, May 9-11, 1995.

[8] Pirzadeh, Shahyar, "Three-Dimensional Unstructured Viscous Grids by the Advancing-Layers Method," AIAA Journal, V ol. 34, No. 1, January 1996, pp. 43-49.

[9] Swanson, R.C., and Rumsey, C.L., "Numerical Issues for Circulation Control Calculations," AIAA Paper 2006-3008, June 2006.

[10] McGowan, Gregory, Rumsey, Christopher, Swanson, R. Charles, and Hassan, Hassan, "A Three-Dimensional Computational Study of a Circulation Control Wing," AIAA Paper 2006-3677, June 2006.